

The Conformation of Fibronectin on Self-Assembled Monolayers with Different Surface Composition: An FTIR/ATR Study

SHIH-SONG CHENG,* KRISHNAN K. CHITTUR,†^{1,2} CHAIM N. SUKENIK,* LLOYD A. CULP,† AND K. LEWANDOWSKA†

Department of *Chemistry and †Molecular Biology and Microbiology, Case Western Reserve University, Cleveland, Ohio, 44106; ‡Chemical Engineering Department, University of Alabama in Huntsville, Huntsville, AL 35899

Received October 19, 1992; July 8, 1993

One aspect of the design of biocompatible synthetic surfaces requires an understanding of both the dynamics of protein interaction and the development of techniques to preferentially control protein adsorption. Our studies focus on self-assembled monolayers (SAMs) that are water stable, highly uniform, and a well-controlled surface composition. These SAMs can be used to modify surface properties of metals, polymers, and many other substrates. We report specific effects of surface functional groups on the spreading and other physiological responses of fibroblasts and neuroblastoma cells. Our studies suggest that surfaces with different compositions modulate the conformation of fibronectin (FN) and thus affect the differentiation responses of fibroblasts and neuronal cells in cell type-specific patterns. Using aqueous Fourier transform infrared (FTIR) attenuated total internal reflection (ATR) techniques we directly evaluate the hypothesis that fibronectin conformation differs on various SAMs, thereby altering binding reactions with cell surface receptors. Our results clearly demonstrate a measure of surface-dependent conformational changes for FN which are correlated by independent biological measurements on cell behavior on these surfaces.

© 1994 Academic Press, Inc.

INTRODUCTION

Several properties of inert biomaterials, including surface chemistry, surface energy, and morphology, have been shown to play crucial roles in biological interactions (1–3). In the field of biomaterials, the nature of the biomaterial surface has been shown to be critical for biocompatibility. It is now well accepted that blood proteins adsorb rapidly to the surface of the biomaterial and this “conditioning” protein layer controls cellular interaction with biomaterials (4–7). Thus, one approach for the design of biocompatible biomaterials utilizes surfaces that will attract specific proteins and maintain those proteins in the desired conformation to effect maximal responses from the desired cell types. This approach to design has been clear for some time now, but imple-

menting such a process has not been easy. This is due in part to the complexity of the biological response and in part to our inability to accurately characterize the surface and monitor events at the protein–material interface under physiological conditions.

Our studies focus on self-assembled monolayers (SAMs) that are water stable, highly uniform, and have a well-controlled surface composition (8). The assembly of artificial layered structures based on the self-association and self-organization of molecules occurring spontaneously at solid–fluid interfaces has been previously described (9). This methodology creates oriented compact monolayers by adsorption of amphiphiles from homogeneous organic solution onto a polar solid surface, thereby modifying surface properties. These films allow different bulk materials to have identical surface properties and we explore their use to regulate cell responses.

Surfactants are synthesized with a SiCl_3 group at one end and an aprotic, chemically manipulable functional group at the other. The SiCl_3 moiety enables covalent attachment of the molecules to surfaces rich in hydroxyl groups, e.g., glass, germanium, etc. These self-assembled organic monolayers are similar in organization and packing to Langmuir–Blodgett (LB) films, but are anchored to the hydroxyl-bearing surfaces by a cross-linked siloxane network. The stability of these films opened the door to the creation and study of new monolayer and multilayer assemblies. LB films, while being uniform and well characterized, require carefully controlled conditions and relatively sophisticated equipment for preparation, and are quite fragile once formed. With SAMs, the assembly is robust and it can be created in an ordinary laboratory environment with no special equipment. A wide range of functionalities can be tolerated in the deposition process and a variety of chemical transformations can be achieved once the monolayer has been deposited. Among the functional groups that can be present (remote from the anchoring functionality) in SAM forming systems are olefins, esters, ethers, nitriles, thioethers, and thioesters. Among the *in situ* transformations reported are the conversion of terminal olefin to alcohol, dibromide, or acid, the conversion

¹ To whom correspondence should be addressed.

² E-mail address: kchittur@ebs330.eb.uah.edu (Internet) uahkxc01@uahvax1.bitnet

of ester to acid or alcohol, the creation of thiols from thio-cyanides or thioacetates, and others (8).

We demonstrate specific effects of surface functional groups on the spreading and other physiological responses of fibroblasts (10–12). Our studies suggest that surfaces with different compositions modulate the conformation of fibronectin and thus affect the differentiation responses of fibroblasts and neuronal cells in cell type-specific patterns. The studies reported herein were undertaken to directly evaluate the hypothesis that fibronectin conformation differs on various SAMs, thereby altering binding reactions with cell surface receptors.

A number of features of these SAMs make them ideal for studying the conformation of adsorbed fibronectin (FN) using FTIR/ATR techniques. These siloxane-anchored SAMs are easily deposited on Ge ATR crystals and are thin (<30 Å), a requirement for FTIR/ATR in protein adsorption studies. Perhaps more importantly, the uniformity, stability, and reproducibility of the SAMs eliminates artifacts due to inconsistent surface preparation or composition.

Our previous studies indicate that fibronectin is very tightly bound to these modified surfaces. Using an ATR flow cell, spectral measurements of the adsorbed FN could therefore be made as the deposition was occurring and after flushing the cell with fresh buffer to remove any loosely adsorbed protein. Spectral data were collected to provide information on both the amounts of protein on the surface and changes in conformation with time.

The Amide I band in proteins represents primarily the C=O stretching vibrations of the amide groups, coupled to the in-plane NH bending and CN stretching modes (13). The exact frequency of this vibration depends on the particular secondary structure adopted by the polypeptide chains. In proteins like fibronectin, one generally finds a number of domains in different conformations. Structure-spectra correlations of Amide I band frequencies with the presence of α -helical, antiparallel and parallel β -sheets and random coil structures were established as a result of a systematic study by Byler, Susi, and co-workers (14–16). These studies were extended by other groups (17–23) including that by Jakobsen who showed that correlations developed for proteins in solution can be used for proteins adsorbed to surfaces. The widths of the Amide I bands assigned to the various secondary structures are large compared to the separation of their peak maxima; thus the Amide I band of complex proteins, like those found in blood, consists of several overlapping bands. Fourier self-deconvolution (FSD) and second derivatives are two algorithms most commonly used to identify the overlapping bands representing α -helices, β -sheets, turns, and other structures in the Amide I band (24, 25). The information provided by such resolution enhancement techniques is strictly qualitative (26). The methodology of curve-fitting first proposed by Fraser and Suzuki can be used for quantitative estimation of protein secondary structure from the

Amide I band (27). The number of component bands and their positions is obtained from resolution enhancement techniques (FSD). An iterative technique is then used to adjust the height and widths of the component bands to “best” fit the overall Amide I contour. Fractional areas of the fitted component bands are then directly related to the relative populations of the conformational structures represented by these components. This method is most useful for following changes in conformation of proteins and less useful for absolute quantitation of protein secondary structure.

Infrared spectra of adsorbed FN on different SAMs were analyzed to reveal both amounts of adsorbed protein and changes in the relative ratios of β -sheet to β -turn structures as a function of time.

EXPERIMENTAL METHODS

Solvents and reagents: Dicyclohexyl (Aldrich) was vacuum distilled and passed through Activity I alumina (3% water by weight). Doubly distilled water was used. Hexadecane was passed through Al₂O₃ to remove polar contaminants. Octadecyl trichlorosilane (Aldrich) was vacuum distilled before use to deposit [CH₃, OTS] surfaces. CHCl₃ (Fisher, HPLC) was used as received. Undecenyl alcohol (Aldrich) was converted into ω -hexadecenyl bromide. This 16-carbon chain with an olefin at one end and a CH₂Br unit at the other was used to make all of the necessary trichlorosilanes. Additional details of these techniques are provided in our earlier publications (8). Fibronectin was purified from human plasma by affinity chromatography and stored in CAPS buffer at –80°C. For adsorption to surfaces, FN was diluted to 20 μ g/ml in phosphate buffered saline.

Self-assembled monolayers: The preparation of the variously functionalized SAM-coated germanium ATR crystals began with the adsorption of surfactants (16 carbon alkyl chains), with SiCl₃ at one end, onto the crystal. All trichlorosilane surfactants were used as 0.02–0.25 M solutions in dicyclohexyl. The SiCl₃ groups provide for the covalent attachment of the molecules to the crystal. Br- and nitrile (CN)-bearing surfaces are directly obtained from deposition of surfactants bearing those functional groups, and the SH-functionalized surface arises from the reduction of either thioacetate or thiocyanate coatings (8). Initially, monolayers are prepared by pipetting 10 ml of the surfactant solution (100 μ l of surfactant in 10 ml of dicyclohexyl) onto one face of the germanium ATR crystal. After 3 min, the solution is removed and the crystal is washed with CHCl₃ and water, and finally with hot CHCl₃. Chemical transformations of the monolayer-coated crystal are done directly on the crystal.

The carboxylic acid (COOH) surface used in this work was obtained by hydrolysis of 17-trichlorosilyl heptadecanoyl chloride (SiCl₃–(CH₂)₁₆–COCl). This preparation differs from the COOH surface used in our earlier FN work (10–12) in that the current surface is less hydrophilic but is more

uniform in bearing only COOH groups on the surface. The surfaces for which data were obtained and analyzed include: Ge (bare, underivatized), Ge/COOH, Ge/Br, Ge/OTS, Ge/SH, and Ge/CN. These surfaces offered a reasonable range of hydrophobicities and chemistries and have convincingly shown that monolayer functionality of various types does not interfere with our measurements on FN.

Contact angle measurements: Contact angle measurements were determined in a Rame-Hart Model 100 contact angle goniometer. Advancing contact angles were determined by watching the advancing periphery of a drop of water placed on the monolayer-covered germanium crystals. Contact angles were measured within 30 s of placement of the drop of water. Receding contact angles were measured as part of the liquid was drawn off. Measurements were made at ambient temperature and the values reported are the average of 4–6 measurements at different points on the surface.

FT-IR/ATR data acquisition: A Digilab FTS-40 with data-collect software in Dr. Roger Marchant's laboratory at Case Western Reserve University was used for these studies. Ge ATR crystals were plasma cleaned and left either uncoated (control) or coated with a SAM monolayer film. Using ATR optics the spectra of the SAMs were obtained; bare germanium ATR crystal was used as the reference. These spectra confirmed the identity and the integrity of the monolayers prior to protein adsorption experiments.

Adsorption of protein to coated and uncoated Ge crystals was followed in time using techniques we have previously published (28). Briefly, two similar ATR crystals, one coated and the other uncoated, were used for assembling the flow cell. Only one flow channel was used during individual adsorption runs. PBS buffer was then introduced into the flow channel and a reference spectrum was obtained. FN solution (20 $\mu\text{g}/\text{ml}$, in phosphate-buffered saline, $\text{pH} = 7.4$, PBS) was introduced into the ATR flow cell, displacing the PBS buffer under which the surface had initially been equilibrated. The flow cell was sealed off and adsorption was allowed to proceed under static conditions, at room temperature. Data collection was initiated immediately. During the first 30 min, spectra were collected every 4 min. All spectra were collected at a resolution of 4 cm^{-1} with one level of zero filling and triangular apodization. During the next 60 min spectra were collected at a slower pace, once every 20 min. A total of 12 spectra were collected during these 90 min. Fresh PBS buffer was then reintroduced to the cell to flush away proteins that were very loosely adsorbed to the surfaces. Two spectra of the strongly adsorbed protein were then obtained during the next 30 min, for a total of 14 spectra. In each experiment, the 14th spectrum thus represented the final spectrum of the adsorbed protein on the surface.

Data processing: Absorbance spectra of proteins were obtained by subtracting the spectrum of buffer (i.e., PBS) by a simple 1:1 rule—except when bands near 1640 cm^{-1}

were investigated. In such cases, the criterion of a flat baseline in the region from 1900 to 1800 cm^{-1} was used for calculating the subtraction factor. The subtraction factor was close to 1.0 in all cases.

The intensity of the Amide II band (1550 cm^{-1}) can be linearly correlated with the total amount of surface-bound protein (29, 30). Actual Amide II intensities were scaled to a water band intensity of 700 milliabsorbance units to correct for experiment-to-experiment variations in alignment and flow-cell assembly. For example, if the intensity at 1640 cm^{-1} for a given experiment was 0.65 absorbance units and the Amide II intensity (after buffer subtraction) was 0.015 absorbance units, the “normalized” value was obtained as $(0.7 \times 0.015/0.65)$ or equal to 0.0162 absorbance units. A detailed discussion of this correction has been published previously (29). Quantitative comparison of protein amounts on ATR surfaces cannot be made without such a correction.

Fourier self-deconvolution (FSD) as described by Kauppinen *et al.* (24) was used to resolve the intrinsically overlapped Amide I spectral region. For adsorbed fibronectin on all the surfaces we examined, FSD analysis revealed three bands in the Amide I spectral region, centered near 1687, 1670, and at 1638 cm^{-1} . The two bands at 1687 and 1670 cm^{-1} represent β -turn structures in the protein and the band at 1638 cm^{-1} reflects β -sheet structures (14–19). There was no evidence of the presence of any α -helical structure; no bands were seen near 1650 cm^{-1} . The relative abundance of sheet and turn structure was obtained by iterative least squares fitting, using the technique described Fraser and Suzuki (27).

The Fraser–Suzuki approach was programmed in Fortran 77 and targeted for the IBM PC (DOS) and compatible environment. The program accepted infrared data files in the J-CAMP format for input. Using initial guesses of peak position (obtained from FSD), peak height (from original spectra) and peak width the program determined how best to fit the Amide I envelope by symmetric Gaussian curves. Best fit was defined in the least-squares sense; the program minimized the difference between the Amide I envelope and that constructed using three symmetric Gaussian curves. During the iterations, the widths, positions, and the intensities of the peaks were allowed to vary from given initial guesses; the program determined the best combination of parameters. The program was allowed to iterate until improvement in the least-squares error was less than 5% of the previous least-squares error. Calculations for all spectra were started using the same initial guesses. The output from the program included peak position, peak intensity, width, and band area. The “percent” secondary structure (β -sheet and β -turn) was calculated from these areas. We have reported changes in these structures both as a function of time and of surface.

A total of 14 spectra were obtained for each experiment on each surface. A minimum of three experiments were done

on each of the six surfaces, using identical data collection techniques. The results from curve fitting were averaged at each time point and standard deviations were computed. Two-tailed Student's *T* test was used to check for significance in the data at the 95% confidence level.

RESULTS AND DISCUSSION

The sessile drop contact angles for the surfaces we studied are shown in Table 1. As expected, bare germanium is hydrophilic (22°) while a $[\text{CH}_3]$ -coated germanium crystal from OTS is most hydrophobic with a water contact angle of 110° . We have previously (10) worked with $[\text{COOH}]$ surfaces having contact angles of 52° . For present purposes we have changed the method of $[\text{COOH}]$ surface generation and observed the relatively higher contact angle of 72° . The more hydrophilic COOH surface is generated by the oxidative cleavage of a terminal olefin with permanganate. These strongly oxidizing conditions produce surfaces that are dominated by COOH groups but also have some other alcohol and carbonyl functionality present. The use of acid chloride hydrolysis (in the present work) guarantees that only acid groups are present. For such surfaces, there are several possible reasons for such a relatively high contact angle. As has been suggested by Ulman and co-workers (31) for alcohol bearing films, the carboxylic acid monolayers, particularly as acid dimers, may reorganize in air and somewhat bury the COOH groups. Similarly elevated contact angles have been seen by other researchers (32) where carboxylic acid terminated symmetrical dialkyl sulfide monolayers on gold show large variations in the contact angle with chain length and where contact angle changes from 40° to 80° have been observed. Since the present work required the creation of surfaces with as uniform as possible array of functionality, these COOH surfaces were used despite their reduced hydrophilicity.

The Amide I and II regions of fibronectin adsorbed to an acid (COOH) surface are shown in Fig. 1. There are two major bands: the Amide I centered near 1640 cm^{-1} and the Amide II, near 1550 cm^{-1} . A plot of the normalized surface adsorbed protein amounts (Amide II, 1550 cm^{-1}) with time for the surfaces studied is shown in Fig. 2. Fibronectin ap-

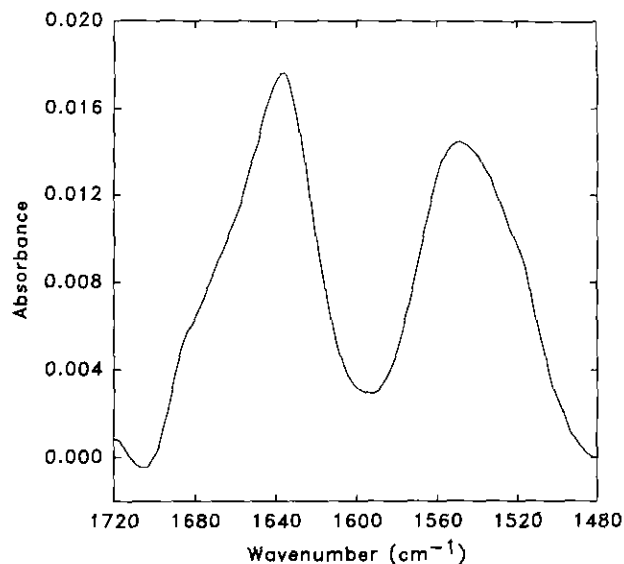


FIG. 1. The Amide I (near 1640 cm^{-1}) and Amide II (near 1550 cm^{-1}) bands of fibronectin adsorbed to a Ge-COOH surface, after subtraction of H_2O .

peared to adsorb at a slower rate on our most hydrophilic surface, bare germanium. The normalized Amide II intensities from the final spectrum for all the surfaces are shown in Table 2. There are no significant differences in the amount

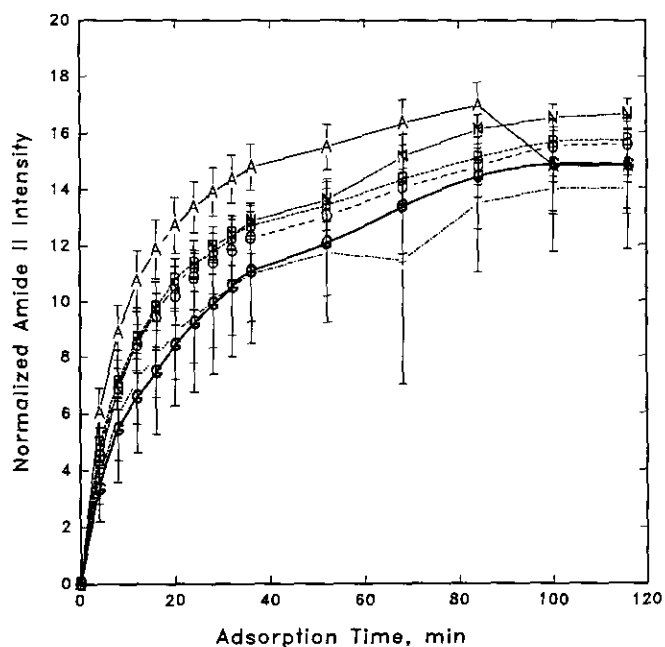


FIG. 2. A plot showing kinetics of fibronectin ($20\text{ }\mu\text{g/ml}$) adsorption to the surfaces we studied, under static conditions using FTIR/ATR. Normalized Amide II intensity versus adsorption time in minutes. Data shown as average (of three experiments) ± 1 standard deviation. (A) Ge-COOH, (N) Ge-CN, (O) Ge-OTS, (B) Ge-bromide, (T) Ge-thiol, and (G) bare germanium.

TABLE 1
Advancing Contact Angles (Average ± 1 Standard Deviation)

Surface	Contact angle
Bare germanium	22 ± 2
Ge-COOH	72 ± 2
Ge-thiol	72 ± 2
Ge-bromide	82 ± 2
Ge-OTS	110 ± 2
Ge-nitrile	77 ± 2

TABLE 2
Normalized Amide II Intensities for Adsorbed Fibronectin
after 116 min (Average \pm 1 Standard Deviation)

Surface	1550 cm^{-1}
Germanium	14.855 \pm 1.57
Acid	14.81 \pm 1.72
Thiol	13.99 \pm 2.13
Nitrile	16.69 \pm 0.53
Bromide	15.73 \pm 0.84
OTS	15.56 \pm 1.09

of protein adsorbed to these surfaces. Our results are in slight contrast to some previous FTIR/ATR studies of fibronectin adsorption on hydrophobic and hydrophilic surfaces (33, 34). These investigators showed that hydrophilic surfaces adsorbed much less protein, at a lower rate, than hydrophobic surfaces. These differences could also reflect the fact that the hydrophilic/hydrophobic nature of surfaces is only one factor that determines the total amount of protein adsorbed to surfaces. Our FTIR/ATR results are consistent, however, with our earlier studies (10–12) on these same surfaces where no differences were seen in total adsorbed protein, quantified by radiolabeling methods.

We then examined the data for surface specific effects on the structure of adsorbed fibronectin. Most studies involving protein secondary structure on surfaces have as a reference the structure of the protein in solution. For many proteins, the principal elements of their structure (α -helix, β -sheet, random coil, aperiodic) can be conveniently analyzed from the circular dichroic contributions of the peptide chromophore in the spectral region from 190–250 nm or by analysis of the Amide I band of proteins in solution. Aqueous solution spectra (free in solution, not adsorbed) of globular proteins like fibronectin cannot be obtained unless their concentration is 10 mg/ml; the intense absorption of H_2O at 1640 cm^{-1} is the primary reason for this limitation. One technique investigators have used to get around this limitation is to dissolve the protein in pure D_2O , but it is difficult to directly relate infrared spectra in D_2O with that obtained in H_2O .

Unlike solution spectroscopy, the ATR technique does not have such a limitation. Since proteins are concentrating at the solid-liquid interface, accurate and precise spectra can be obtained from very low bulk concentrations of protein at submonolayer to multilayer coverages of the surface. Fibronectin is a trace plasma protein and was purified from plasma by affinity chromatography. Attempts were made to obtain a solution infrared spectrum of the stock solution of fibronectin stored in CAPS buffer, but the concentration level was too low and the absorption of H_2O at 1640 cm^{-1} could not be adequately subtracted out. We are thus limited to using information about the solution structure of fibronectin from limited circular dichroic studies. There is general agreement that fibronectin does not contain appreciable

amounts of α -helix because the characteristic double peak at 210 and 222 nm is not present in the spectra (35). Qualitatively, the observed bands at 215 and 200 nm are consistent with the presence of β -sheet. Using completely deuterated water (D_2O) Koteliensky *et al.* (36) have estimated about 25% antiparallel β -sheet in plasma fibronectin using infrared spectroscopy.

In Fig. 3 we show a typical resolution of the Amide I band into the three symmetric Gaussian curves as calculated by the curve-fitting program. Such a resolution was obtained on all 14 spectra, for all replicate experiments, on all the surfaces we tested. We queried the data using two methods. For each data set, at each time point, a ratio of the β -sheet structure (1638 cm^{-1}) to the β -turn structure (1670 cm^{-1}) was calculated using the area ratio of the fitted Gaussian curves at 1638 and 1670 cm^{-1} . The change in this ratio as a function of time and for all the surfaces we examined is shown in Fig. 4a. This ratio changes from approximately 1.5 to about 3.5 during the 2 h of adsorption, suggesting that fibronectin conformation changes with time. This change in structure appears to level off after about 30 min of adsorption on all the surfaces. The increase in ratio suggests that with time, there is an increase in the relative amount of β -sheet to turn type of structure in adsorbed fibronectin. The change in this ratio during the first 40 min is shown separately in Fig. 4b; while there appears to be an early separation of Germanium and acid surfaces from the others, these differences are not statistically significant. In a related study of fibronectin adsorption to polyurethanes, similar observations were made: the ratio of 1634 cm^{-1} peak to the 1670 cm^{-1} peak was observed to increase with increasing protein adsorption (30).

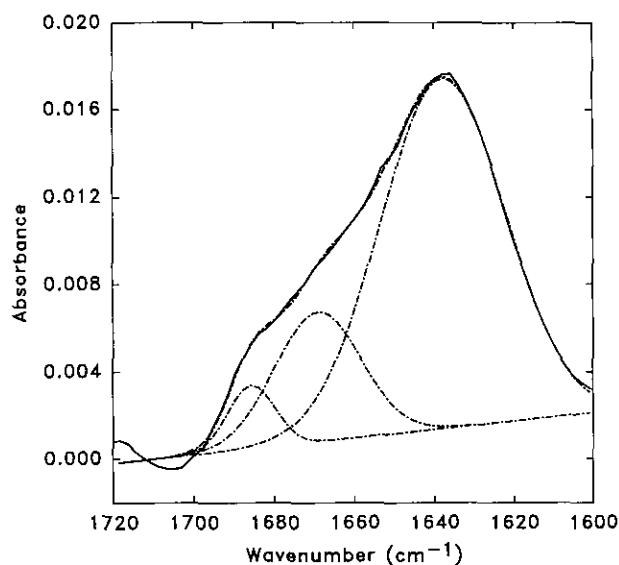


FIG. 3. The Amide I region of fibronectin adsorbed to α -Ge-COOH surface and results from curve fitting (dotted curves).

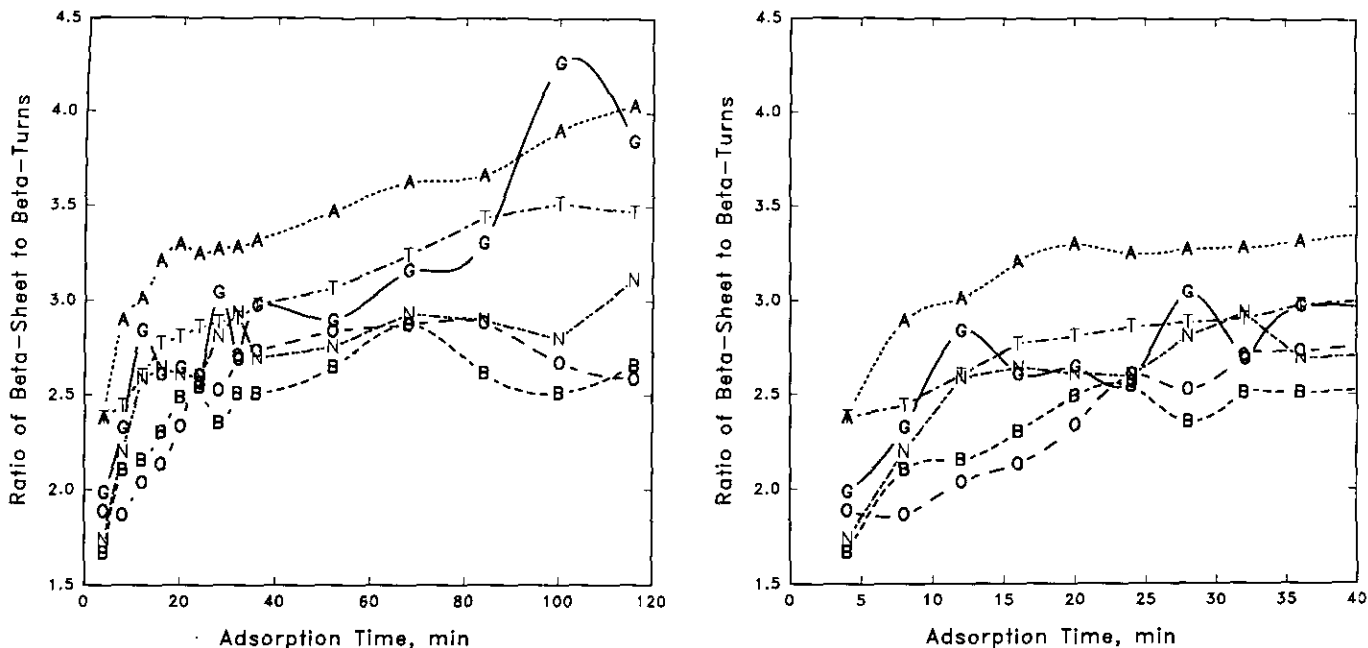


FIG. 4. (a) A plot showing how the ratio of beta-sheet to β -turn bands change with time on the surfaces studied. Since a ratio is plotted, no error bars are shown. (A) Ge-COOH, (N) Ge-CN, (O) Ge-OTS, (B) Ge-bromide, (T) Ge-thiol, and (G) bare germanium. (b) Data from (a) shown for the first 40 min only.

The FT-IR/ATR technique gives us information about the entire adsorbed layer. A spectrum obtained after 10 min of adsorption, for example, represents the "averaged" spectrum of many hundreds of molecules of fibronectin on the surface. The initial layer of proteins, if they are denatured, may retain that changed structure as more fibronectin molecules continue to adsorb. As the surface fills up, proteins will adsorb to other adsorbed protein molecules and are more likely to retain their native structure. Thus, with time, the ratio of native to denatured protein is expected to increase. This is what is expressed in Fig. 4. We have, however, a measure of the total amount of protein on the surface as a function of time: the intensity of the Amide II band. We can thus plot the ratio of native to denatured protein as a function of total adsorbed protein, shown in Fig. 5, and this shows the same trend. Absolute values of the percent areas for the curve-fitted bands at 1687, 1670, and 1638 cm^{-1} are given for all the surfaces as a function of time in Table 3.

We have tabulated separately (Table 4) the average percent areas for the final protein spectra; 116 minutes into the adsorption. Using the two-tailed Student's *T* test, we examined the data for significant differences at the 95% level. There were no significant differences in the structure of adsorbed fibronectin on Germanium and acid surfaces. We could detect no differences between fibronectin on OTS and Bromide surfaces. The structure of adsorbed fibronectin on Ge and acid was significantly different from that adsorbed to OTS and Bromide. As the data in Table 3 show, Thiol and Nitrile surfaces fell somewhere in between. These data show clearly

that different chemical end groups on the substratum modulate fibronectin conformation but have no effect on the amounts bound. These studies support the hypothesis evolved from earlier studies on the evaluation of neurite out-

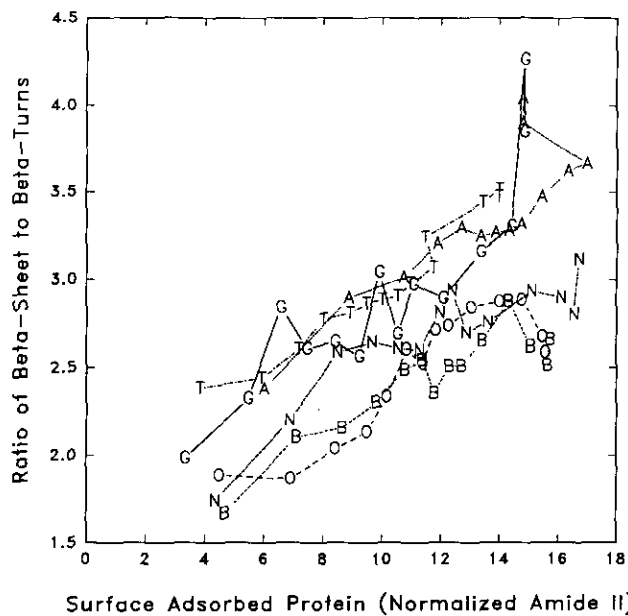


FIG. 5. A plot showing how the ratio of β -sheet to β -turn changes with total amount of adsorbed fibronectin. (A) Ge-COOH, (N) Ge-CN, (O) Ge-OTS, (B) Ge-bromide, (T) Ge-thiol, and (G) bare germanium.

TABLE 3
Curve-Fitting Results

Min	1687	Standard deviation	1670	Standard deviation	1638	Standard deviation
Fibronectin on Germanium						
4	8.42	2.12	30.68	4.31	60.88	4.82
8	7.79	0.76	27.74	2.99	64.47	3.74
12	8.03	1.63	24.27	3.24	68.89	3.14
16	6.26	1.09	26	6.08	67.73	5.08
20	5.64	1.01	25.9	3.65	68.43	3.77
24	5.29	2.26	26.58	4.09	68.12	4.11
28	6.26	0.73	23.2	4.53	70.53	5.19
32	5.69	0.39	25.58	4.35	68.72	4.46
36	6.58	1.06	23.52	2	69.88	3.04
52	6.38	1.3	24.05	3.85	69.56	5.14
68	6.58	2	22.54	3.19	71.17	5.15
84	7.18	3.43	22.2	4.93	73.35	0.1
100	5.4	0.21	17.98	3.52	76.61	3.74
116	5.1	2.26	19.58	5.54	75.31	3.8
Fibronectin on OTS						
4	7.38	3.5	32.09	5.16	60.52	2.94
8	4.23	2.2	33.42	7.15	62.34	5.25
12	4.14	2.05	31.57	8.21	64.29	6.19
16	4.2	2.02	30.6	5.93	65.21	3.98
20	4.82	0.57	28.56	3.18	66.63	2.72
24	5.28	0.23	26.31	1.21	68.42	1.28
28	4.92	0.1	26.99	2.69	68.08	2.65
32	5.69	0.66	25.45	1.58	68.86	2.14
36	5.39	0.34	25.35	2.3	69.27	2.39
52	5.26	0.4	24.69	0.97	70.04	1.32
68	5.17	0.38	24.5	0.82	70.33	1.1
84	5.32	0.48	24.39	1.34	70.28	1.58
100	5.37	0.54	25.78	1.54	68.85	1.64
116	4.64	1.02	26.61	2.67	68.75	2.07
Fibronectin on Bromide						
4	4.69	0.63	36.21	6.59	60.42	5.2
8	4.74	0.39	30.71	3.67	64.58	3.57
12	4.95	0.49	30.14	2.17	64.91	1.71
16	5.21	0.86	28.72	2.63	66.07	1.77
20	5.05	0.3	27.24	2.92	67.71	2.67
24	5.2	0.57	26.77	3.3	68.03	2.76
28	4.96	0.89	28.37	1.99	66.68	1.15
32	4.96	0.44	27.11	1.57	67.93	1.15
36	5.02	0.81	27.08	1.68	67.9	0.98
52	5.26	0.54	25.98	1.04	68.76	0.53
68	4.98	0.72	24.53	2.44	70.49	2.44
84	5.02	0.54	26.27	0.36	68.7	0.18
100	4.78	0.52	27.12	1.23	68.1	0.82
116	4.7	0.63	26.07	2.02	69.23	1.42

growth by neuroblastoma cells (10). Fibronectin at the concentrations used in this study was adsorbed to derivatized glass cover slips for about 1 h, at 37°C. Platt neuroblastoma cells were then added and allowed to attach and spread for 16 h. The cells were then fixed with glutaraldehyde and the

neurites generated were quantitated by techniques described previously. While there was poor cytoplasmic spreading and virtually no neurites formed on hydrophobic surfaces like Bromide and OTS, significantly greater neurite outgrowths were observed on acid and SiOH (bare glass) substrates. In-

TABLE 3—Continued

Min	1687	Standard deviation	1670	Standard deviation	1638	Standard deviation
Fibronectin on Nitrile						
4	6.18	3.86	34.26	6.11	59.56	3.48
8	5.9	0.64	29.42	1.94	64.68	1.4
12	6.24	0.34	26.15	1	67.61	1.24
16	5.78	0.17	25.89	1.26	68.34	1.12
20	5.97	0.1	26.07	2.02	67.97	2.12
24	5.8	0.31	26.2	1.09	68.01	1.4
28	5.48	0.53	24.82	2.2	69.7	2.71
32	5.73	0.85	23.96	1.43	70.31	1.88
36	5.49	0.21	25.59	1.93	68.91	2.1
52	5.13	0.51	25.28	2.75	69.6	2.64
68	5	0.71	24.18	4.83	70.82	4.71
84	5.4	0.3	24.28	2.72	70.31	2.44
100	4.97	1.07	25.02	3.9	70	2.85
116	5.52	0.27	22.97	0.91	71.5	1.1
Fibronectin on Acid						
4	8.33	0.89	27.14	2.13	64.52	2.39
8	6.75	0.7	23.95	1.16	69.29	1.83
12	6.36	0.44	23.35	1.06	70.3	1.49
16	6.39	0.28	22.27	0.97	71.35	1.17
20	6.23	0.44	21.83	1.29	71.95	1.52
24	6.11	0.44	22.11	0.72	71.78	1.12
28	6.08	0.35	22	0.68	71.91	0.9
32	5.98	0.33	21.97	2.05	72.05	2.25
36	5.88	0.38	21.58	1.04	71.53	1.11
52	5.81	0.44	21.07	2.02	73.12	2.29
68	5.6	0.53	20.42	2.62	73.98	3.07
84	5.49	0.61	20.27	1.5	74.24	1.8
100	4.93	0.33	19.41	0.97	75.66	1.1
116	4.8	0.36	18.89	1.49	76.3	1.45
Fibronectin on Thiol						
4	15.74	9.04	24.93	10.46	59.34	5.75
8	8.42	2.61	26.62	5.42	64.95	3.76
12	7.27	0.96	25.75	2.91	66.98	2.53
16	6.68	0.84	24.76	1.71	68.57	1.04
20	6.18	0.2	24.64	0.85	69.18	0.88
24	6.42	0.68	24.25	1.12	69.33	1.05
28	6.09	0.25	24.19	0.72	69.72	0.77
32	5.93	0.17	24.1	0.95	69.97	0.98
36	5.91	0.14	23.67	0.89	70.43	0.93
52	5.84	0.08	23.16	0.64	70.99	0.66
68	5.62	0.06	22.27	1	72.11	0.95
84	5.5	0.03	21.29	1.36	73.21	1.38
100	5.32	0.4	20.98	0.68	73.7	0.61
116	5.32	0.24	21.18	0.65	73.49	0.48

Note. Percent areas (average and standard deviation) for bands at 1687, 1670, and 1638 (cm^{-1}) wavenumbers as a function of time.

terestingly, neurite formation on Bromide and OTS could be "rescued" if the initial fibronectin adsorption was done in the presence of excess albumin, preserving its conformation on such hydrophobic substrates.

SUMMARY

This study shows that the effect of modification of the surface chemistry on the attachment and the spreading of

TABLE 4

Percent Areas Calculated from Curve Fitting (Average \pm Standard Deviation) for Adsorbed Fibronectin after 116 Min (Average \pm 1 Standard Deviation)

Surface	1687 cm ⁻¹	1670 cm ⁻¹	1638 cm ⁻¹
Germanium	5.1 \pm 2.26	19.58 \pm 5.54	75.31 \pm 3.8
Acid	4.8 \pm 0.36	18.89 \pm 1.49	76.3 \pm 1.45
Thiol	5.32 \pm 0.24	21.18 \pm 0.65	73.39 \pm .48
Nitrile	5.52 \pm 0.27	22.97 \pm 0.91	71.5 \pm 1.1
Bromide	4.7 \pm 0.63	26.07 \pm 2.02	69.23 \pm 1.42
OTS	4.64 \pm 1.02	26.61 \pm 2.67	68.75 \pm 2.07

Note. Values obtained from Table 3.

fibroblasts on surfaces can be described in terms of the conformational properties of fibronectin and not by the total amount of fibronectin adsorbed. The FTIR/ATR approach clearly demonstrated a measure of surface-dependent conformational changes for FN which are correlated by independent biological measurements on cell behavior on these surfaces. This study thus holds promise that we may be able to directly correlate adhesive protein activity to its surface-bound conformation.

ACKNOWLEDGMENTS

This work was supported by the U.S. National Institutes of Health, HL-38936 (Chittur), CA-27755, and NS 17139 (Culp), the Edison Biotechnology Center (Culp and Sukenik), and the University of Alabama in Huntsville (Chittur). We thank Dr. Roger E. Marchant of the Biomedical Engineering Department at Case Western Reserve University for the use of his FTIR equipment.

REFERENCES

- Ratner, B. D., Johnston, A. B., and Lenk, T. J., *J. Biomed. Mater. Res.: Appl. Biomater.* **21**, 59 (1987).
- Andrade, J. D., "Surface and Interfacial Aspects of Biomedical Polymers, Vol. 1: Surface Chemistry and Physics," Plenum, New York, 1985.
- McIntire, L. V., Addonizio, V. P., Coleman, D. L., Eskin, S. G., Harker, L. A., Kardos, J. L., Ratner, B. D., Schoen, F. J., Sefton, M. V., and Pitlick, F. A., "Guidelines for Blood-Materials Interactions-Devices and Technology Branch," NIH Publication No. 85-2185 (revised), Division of Heart and Vascular Diseases, National Heart, Lung and Blood Institute, U.S. Department of Health and Human Services, Washington, DC, July 1985.
- Vroman, L., Adams, G. L., and Fischer, G. C., *Adv. Chem. Ser.* **199**, 265 (1982).
- Wojcicichowski, P., Ten Hove, P., and Brash, J. L., *J. Colloid Interface Sci.* **111**, 555 (1986).
- Slack, S. M., and Horbett, T. A., *J. Colloid Interface Sci.* **133**, 148 (1989).
- Horbett, T. A., *J. Biomed. Mater. Res.* **15**, 673 (1981).
- Balachander, N., and Sukenik, C. N., *Langmuir* **6**, 1621 (1990).
- Netzer, L., and Sagiv, J., *J. Am. Chem. Soc.* **105**, 674 (1983).
- Lewandowska, K., Balachander, N., Sukenik, C. N., and Culp, L. A., *J. Cell. Physiol.* **141**, 334 (1989).
- Sukenik, C. N., Balachander, N., Culp, L. A., and Lewandowska, K., *J. Biomed. Mater. Res.* **24**, 1307 (1990).
- Lewandowska, K., Pergament, E., Sukenik, C. N., and Culp, L. A., *J. Biomed. Mater. Res.* **26**, 1343 (1992).
- Miyazawa, T., Shimanouchi, T., and Mizushima, S. I., *J. Chem. Phys.* **24**, 408 (1956).
- Yang, W., Griffiths, P. R., Byler, D. M., and Susi, H., *Appl. Spectrosc.* **39**, 282 (1985).
- Byler, D. M., and Susi, H., *Biopolymers* **25**, 469 (1986).
- Susi, H., and Byler, D. M., *Appl. Spectrosc.* **42**, 819 (1988).
- Jakobsen, R. J., and Wasacz, F. M., *ACS Symp. Ser.* **343**, 339 (1987).
- Jakobsen, R. J., Wasacz, F. M., Brash, J. M., and Smith, K. B., *Biopolymers* **25**, 639 (1986).
- Wasacz, F. M., Olinger, J. M., and Jakobsen, R. J., *Biochemistry* **26**, 1464 (1987).
- Anderle, G., and Mendelsohn, R., *Biophys. J.* **52**, 69 (1987).
- Kato, K., Matsui, T., and Tanaka, S., *Appl. Spectrosc.* **41**, 861 (1987).
- Koenig, J. L., and Tabb, D. L., in "Analytical Applications of FT-IR to Molecular and Biological Systems" (J. R. Durig, Ed.), p. 241, J. Reidel, Boston, 1980.
- Kirsch, J. L., and Koenig, J. L., *Appl. Spectrosc.* **43**, 445 (1989).
- Kauppinen, J. K., Moffatt, D. J., Mantsch, H. H., and Cameron, D. G., *Appl. Spectrosc.* **35**, 271 (1986).
- Cameron, D. G., and Moffatt, D. G., *J. Test. Eval.* **12**, 78 (1984).
- Surewicz, W. K., and Mantsch, H. H., *Biochim. Biophys. Acta* **952**, 115 (1988).
- Fraser, R. D. B., and Suzuki, E., in "Physical Principles and Techniques in Protein Chemistry," Part B, (S. J. Leach, Ed.), p. 213, Academic Press, 1970.
- Chittur, K. K., Fink, D. J., Leininger, R. I., and Hutson, T. B., *J. Colloid Interface Sci.* **111**, 419 (1986).
- Fink, D. J., Hutson, T. B., Chittur, K. K., Leininger, R. I., and Gendreau, R. M., *Anal. Biochem.* **165**, 147 (1987).
- Fink, D. J., and Gendreau, R. M., *Anal. Biochem.* **139**, 140 (1984).
- Tillman, N., Ulman, A., and T. L. Penner, *Langmuir* **5**, 101 (1989).
- Troughton, E. B., Bain, C. D., Whitesides, G. M., Nuzzo, R. G., and Allara, D. L., *Langmuir* **4**, 365 (1988).
- Pitt, W. G., Spiegelberg, S. H., and Cooper, S. L., *ACS Symp. Ser.* **343**, 324 (1987).
- Giroux, T. A., and Cooper, S. L., *J. Colloid Interface Sci.* **139**, 351 (1990).
- Odermatl, E., and Engel, J., in "Fibronectin" (D. E. Mosher, Ed.), p. 25, Academic Press, 1989.
- Kotliansky, V. E., Glukhova, M. V., Bejanian, M. V., Smirnov, V. N., Filimonov, V. V., Zalite, O. M., and Venyaminov, S. Y., *Eur. J. Biochem.* **119**, 619 (1981).